Analysis of Danger Posed by Near-Earth Asteroid 1994 PN

Amy Dai, Frank Bu, Aaron Kogan.
Leitner Family Observatory and Planetarium, New Haven, CT

KEYWORDS. Asteroid, astrophysics, orbit determination

BRIEF. Analyze the orbit of asteroid 1994 PN to predict its potential of colliding with Earth.

ABSTRACT. In space, many near-earth asteroids are considered "killer asteroids" because of their possibility of colliding with the Earth. This paper details the methods of data collection and analysis, orbit modelling, and model optimization for the Near-Earth Asteroid (NEA) 1994 PN in order to determine its level of danger to the Earth. Telescopes at the Leitner Family Observatory (LFO) in New Haven, Connecticut; Mayhill, New Mexico; and Sierra Nevada Mountains, California were operated both locally and remotely to take images and collect astrometric and photometric data on 1994 PN. The data was filtered through the Method of Gauss to calculate the preliminary orbit of the asteroid. Data was then iterated through a genetic algorithm program to optimize the orbit model to achieve best. Finally, a Rebound long-term integrator extrapolated the optimized orbit model to ascertain the orbit of 1994 PN in the distant future. Our study found that 1994 PN has osculating orbit elements of semi-major axis (a) 2.351 AU, eccentricity (**e**, in AU) <0.405, -0.169, -0.315>, inclination angle (i) 45.8°, longitude of the ascending node (Ω) 113.1°, and argument of the perihelion (ω) 234°. These elements indicate a moderately elliptical orbit significantly offset from the Earth's plane of orbit. The final iteration of the model optimization procedure yielded an uncertainty in our results of rms_{RA} = 0.033° and an rms_{Dec} of 0.039°. The simulation shows that there is a high possibility of collision between 1994 PN and Earth.

INTRODUCTION.

The Value of Studying Near-Earth Asteroids.

Near-Earth asteroids (NEAs) are usually main-belt asteroids that, through gravitational perturbations, experience close encounters with the Earth. Due to their relative proximity, further gravitational disturbances can cause collisions. Historically, NEAs and other earth-crossing objects (such as comets) have produced Earth's approximately 120 meteorite impact craters, including the impact at the K/T boundary approximately 65 million years ago which resulted in a mass extinction of 90% of all species [1]. In addition, NEAs could be readily accessed for resource extraction. Metallic asteroids contain precious metals (e.g. gold, platinum, and platinum-group metals) and semiconductors (used in the manufacture of technology products) in concentrations higher than what is available on Earth [6]. NEAs also carry non-metallic materials, such as nitrogen, oxygen, water, clays, hydrated salts, and hydrocarbons. Water, believed to be found on approximately 50% of NEAs, is a particularly useful and readily extracted resource [6].

Current Tracking Methods.

The first step in collecting data on and determining the orbit of a specific NEA is to be able to reliably track the asteroid through its orbit to effectively direct the telescope for imaging. One ongoing effort to track NEAs is the Near-Earth Asteroid Tracking (NEAT) system, which has operated autonomously at the Maui Space Surveillance Site since December 1995. NEAT has contributed to the data available on more than 1,500 minor planets and detected more than 26,000 main-belt asteroids. In addition, NEAT is an efficient detector of near-earth asteroids larger than 1 km in diameter. The data NEAT has collected has enhanced the body of knowledge used to evaluate the hazard of Near-Earth objects and calculate the target location of an object for future space missions [5].

NASA also has a joint effort with the Marshall Space Flight Center (MSFC) and Jet Propulsion Laboratory (JPL) to create the "NEA Scout" program, a concept that would use inexpensive CubeSats, a type of "miniature or nanosatellites created for research use, to encounter NEAs. The NEAScout program seeks to explore less-known small NEAs (diameters in the 1-100 m range) and provide information for the Asteroid Redirect Mission (ARM), a planetary defense program, as well as identify all asteroid threats for the Asteroid Grand Challenge [7].

Recently, new methods of tracking asteroids have arisen, such as the "synthetic tracking" methodology presented by Shao [7]. Synthetic tracking is a useful tool for documenting small, dim, and quickly moving NEAs. It relies on the use of high speed cameras and data processing by employing a sophisticated "shift and add" technique to synthetically layer images on top of one another to produce a simulated long-exposure shot of the NEA under observation [7].

Mechanics of Orbit Determination.

Orbits of a celestial object can be determined from its initial heliocentric position vector, r, and its velocity vector, ṙ. The force of gravity acts between other celestial objects and the one of interest. For this project, the forces of gravity on the asteroid by objects other than the Sun, Earth, Jupiter, and Mars are negligible. The acceleration due to gravity is determined by Newton's Gravitational Law: $\ddot{\vec{r}} = \frac{-\mu \vec{r}}{r^3}$. Furthermore, total energy is conserved throughout the asteroid's orbit, and the asteroid behaves according to Kepler's Laws of Planetary Motion. The resulting motion follows the Conic Section Law with the Sun at one focus and perturbations by other objects [3]. As the position vector (**r**) of the asteroid changes, its net acceleration will change, thus affecting its velocity (ṙ). Computer integrators with short time steps can accurately approximate the asteroid's orbit to a reasonable accuracy using these physical laws.

To solve for r and ṙ, the fundamental vector triangle is considered. The distance from the observer to the asteroid is defined as ρ (the range); the unit vector pointing from the observer to the asteroid is defined as $\hat{\rho}$; the vector pointing from the observer to the sun is defined as **R**; the vector pointing from the sun to the asteroid is defined as **r**. (Figure 1). By performing the Method of Gauss around a middle observation to solve for p, the preliminary vector orbital elements in ecliptic coordinates (a coordinate system with the plane of Earth's equator as the x-y plane, and Earth's axis of rotation as the z-axis) are determined: the position vector **r** and the velocity vector ṙ. These two vectors are needed for initial orbit determination (defining the asteroid's orbit by the classical orbital elements; Figure 2).

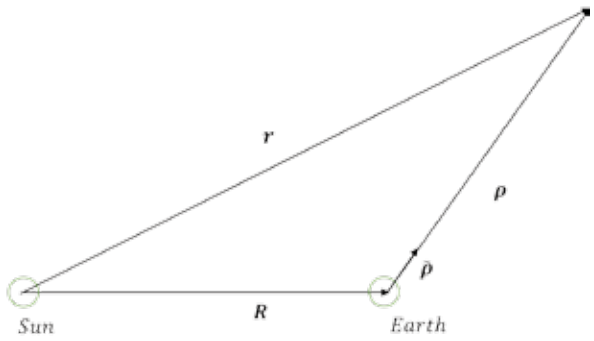

Figure 1. The fundamental vector triangle of positions of the Sun, the Earth, and the Asteroid.

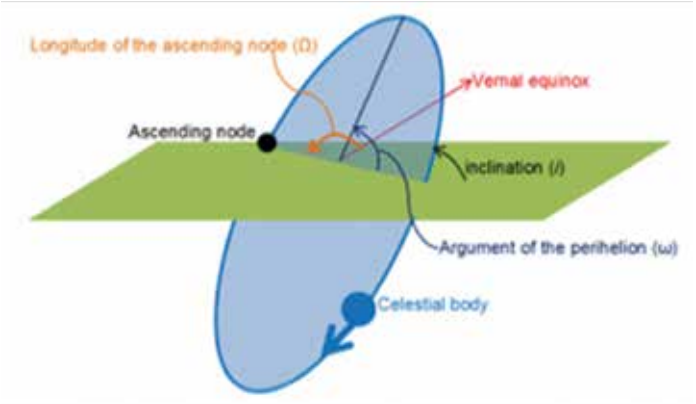

Figure 2. A depiction of the classical orbital elements.

With an initial orbit, the model was optimized (fitted) to our observed data using the genetic algorithm process. With various mapping techniques and a standard to evaluate fitness, a genetic algorithm can be used to evolve a solution to match various demands, including optimization of a model [4]. The genetic algorithm program used here generated asteroid candidates in a Gaussian distribution of position and velocity vectors around the initial asteroid defined by r2 and ṙ2 from the Method of Gauss. For each of the candidates, coordinate positions Right Ascension (RA; a measure of celestial "longitude") and Declination (Dec; a measure of celestial "latitude") were interpolated to all of the observation dates. Each candidate's set of predicted RA and Dec data was then compared with our observation data (the asteroid's observed RA and Dec). By calculating the root mean square (rms; a measure of the predicted data's deviation from the observed data), the best fit candidate with the lowest rms was found within this generation. Its values of r and ṙ become the center of the Gaussian distribution for the next generation of asteroid candidates. After several generations, the candidate with the minimum rms was found, and its values of r and ṙ became the basis for the "optimized" orbit model.

MATERIAL AND METHODS.

Data Collection.

The local 16-inch telescope at the Leitner Family Observatory in New Haven, CT was used. In order to maximize data collection in a limited amount of time, remote telescopes (T21 and T24 in New Mexico and California, respectively, available on itelescope.net) were also employed. For both the local and New Mexico observations, exposure times of 60 seconds were used because these two telescopes have a smaller light-collecting surface area; four sets of nine images in alternating series of luminance and red filters were taken. The luminance filter images were used for astrometry (the process of calculating the object's RA and Dec coordinates using reference stars) because the luminance filter allows more light passage than other filters, so the asteroid appears brighter and the asteroid's centroid (pixel location on the image) more easily measured. The red filter images were used for photometry (the process of calculating the object's brightness) in order to minimize the signal-to-noise ratio. For the California observations, exposure times of 30 seconds were utilized (the California telescope has a larger collecting lens, and longer exposure times would have saturated the pixels of the CCD camera); the same setup of four sets of nine images in alternating luminance and red filters was used. Eight total collections of images were taken in these three locations throughout the four weeks spanning July 10 and August 7, 2016.

Astrometry.

Images from each evening were first analyzed using Maxim DL (an astronomical image processing tool) in order to locate the asteroid. Each series of nine images from the same filter was first calibrated by subtracting the flat-field, then aligned, and finally combined in groups of three. Then, Maxim DL's "blink" function was used to rapidly switch between the combined images at 0.2 to 0.5 seconds per frame and locate the asteroid. During the blink process, the asteroid would appear as a small Gaussian, moving relative to the background stars. The located asteroid was marked with a white ring using Maxim DL's "annotate" function.

Once the asteroid was found and marked, the combined images were uploaded to astrometry.net. This online software matched the reference stars in the images, along with their RA and Dec coordinates, to known coordinates from star catalogs. With these reference coordinates, the astrometry.net program then attached RA and Dec coordinates to each pixel value in the image. A new image was created with overlaid RA and Dec coordinates, and the image and its information were downloaded as a .fits file. Then, DS9 (an astronomical imaging and data visualization application) was used to find the ICRS (International Celestial Reference System; a standardized celestial coordinate system) RA and Dec of the centroid of the asteroid.

Photometry.

Each photograph was further analyzed using DS9's optical catalog UCAC4 to calculate the asteroid's apparent magnitude. Arbitrary stars with known red magnitudes ("rmag"; a measure of the apparent brightness of an object's red wavelengths only, as seen from Earth) were selected as reference stars in the Maxim DL photometry program. Then, the red magnitude of the asteroid in one image was calculated within the Maxim DL program using the reference magnitudes. Several red magnitudes were averaged to produce a single apparent magnitude for our asteroid on a particular night of observation. This process was repeated for each of the remaining series of observations; the resulting apparent magnitudes, as well as the RA-Dec coordinates found in the above section "Astrometry," comprise the observed data of the asteroid detailed in Supplement Table 1.

Using Photometry to Find Size.

From the asteroid's apparent magnitude, the asteroid's diameter can be determined. The equation $\Delta M = -2.5\log\left(\frac{p_1}{p_2}\right)$ yields a magnitude "increment". Adding the ΔM to the apparent magnitude yields the *absolute* magnitude. Using the calculated *absolute* magnitude, we can use the following equation to calculate the diameter of the asteroid: $D = \frac{1329}{\sqrt{p}} 10^{-0.2H}$ where D is diameter in km, *p* is the albedo (guessed due to the inability to measure it directly with the equipment available), and *H* is the apparent magnitude.

Using Astrometry for Initial Orbit Determination.

The RA and Dec coordinates of the asteroid at particular times was recorded according to the procedure outlined in the "Data Collection" and "Astrometry" sections. To determine the initial orbit (which would later be fitted to observed data using genetic algorithm model optimization techniques), it is necessary to find the topocentric range vector, **ρ**, the vector from the observer's location to the asteroid. The most straightforward way to accomplish this is through parallax calculations conducted in significantly distant locations during overlapping times. However, due to weather conditions, we could not acquire simultaneous data. Therefore, the Method of Gauss was employed to find the heliocentric position (**r**) and velocity ($\dot{\mathbf{r}}$) vectors of the asteroid. Three data points were used in Method of Gauss calculations to solve for the position and velocity vectors at the time of the middle observation (T) of the set of three observations.

For detailed description of Method of Gauss, please see supplement material.

RESULTS.

To validate our observation data, we compared our calculated (observed) values of RA and Dec and orbital elements on July 23, 2016 (JD 2457592.6545) to those of JPL's ephemeris for the same time. The comparison showed that our observation data is accurate (Supplement Table 2). Thus, we consider our observed values acceptable for calculation and data analysis (within 0.1 to 0.01 of the ephemeris values, except for the measurements of apparent magnitude). The uncertainty in our measurements is the value of rms, which equals 0.0025.

For the three sets of observation data required in the method of Gauss calculation, we used our data collected at time JD 2457586.7092, JD 2457592, and JD 2457597 (observations about 5 to 6 days apart from each other). We tried to maximize the time gap between these three observations to maximize the change in the asteroid's position vector. After performing genetic algorithm model optimization, the optimum heliocentric position vector was found to be:

$\mathbf{r}$ = <0.234, -1.402, -0.241>

And the optimum heliocentric velocity vector was:

$\dot{\mathbf{r}}$ = <0.592, 0.598, -0.504>

With these vectors, we calculated the classical osculating orbital elements for JD 2457592.6773, summarized below in Table 1.

Table 1. Calculated results of classical osculating orbital elements for JD 2457592.6773.

a (AU)	e (AU)	i	Ω	ω
2.351	<0.405, -0.169, -0.315>	45.8°	113.1°	234.4°

Long-term integration of the asteroid's orbit using the Rebound computer integrator to predict future orbital paths showed periodically varying distances between 1994 PN and the Earth (Figure 3). However, as shown in Figure 4, the asteroid will come dangerously close to the Earth (on the order of hundredths of an AU) around year 4157. Although step-wise computerized integrators do accumulate some error, our results are justified because of the small (less than 0.01) value of the rms obtained after genetic algorithm model optimization and the accuracy of our calculated and observed data (Supplement Table 2). Furthermore, the periodicity of the asteroid's distance from Earth and the dramatically close encounter in the year 4157 show overall trends in the orbit of 1994 PN—trends which would hold due to their intrinsic natures despite fluctuations in exact motion and imperfect orbital integration. We can expect with little uncertainty (based on the small rms) that the orbit of NEA 1994 PN will bring it close to Earth (less than 1.75 AU) about every 49 years and extremely close to Earth around the year 4147.

DISCUSSION.

Potential Damage of Collision.

1994 PN has a calculated diameter of 1.06 to 1.84 km, so it would do considerable damage if it crashed into the Earth. Using the calculator provided by Earth Impact Effect Program run by Purdue University and Imperial College London, we estimated the crater diameter caused by such an impact to be 13.6 km. However, the impact would not have enough momentum to cause a mass extinction or widespread death.

Explanation of Brightness Fluctuations.

In addition to periodic distance-to-Earth fluctuations between 2 AU and 4 AU, the data table of our observations also indicates changing brightness levels (see "AP Mag" column of Supplement Table 1). This occurrence can be most likely explained by asteroid tumbling during orbit. Apparent magnitude measurements that change over time reveal the way the asteroid is rotating (or "tumbling" through space), and thus, the shape of the asteroid. For example, if the apparent magnitude remains relatively constant for long periods of time, then the asteroid might be rotating on an approximate axis of symmetry. On the other hand, if the apparent magnitude fluctuates greatly so that the asteroid becomes dramatically brighter or dimmer as time passes, then the asteroid might be oblong-shaped and rotating so that we see the small face of the ovoid illuminated by the Sun (small reflective surface area; dim), and then the long face illuminated by the Sun (large reflective surface area; bright). Therefore, if the asteroid was rotating along the different ovoid faces, the observed apparent magnitude would fluctuate over time.

Improvements Upon the Study.

Given more time, we could capitalize on the changing magnitudes by observing the asteroid with radio waves and constructing a model of its shape. This project could also be extended by analyzing the asteroid's reflection spectrum to determine its surface composition and economic viability for exploration and resource collection.

To further improve upon the study, we would like to try parallax observations again for initial orbit determination. On the evening of July 25, 2016, simultaneous observations were attempted in collaboration with Blasy *et. al.*, during which we would observe remotely from the New Mexico and Blasy *et. al.* would observe using the local Leitner Family Observatory telescope. However, due to inclement weather which delayed data collection at the local observation station, we were unable to gather images taken at coinciding times; the first image from the local observations was taken five minutes after the last image from the New Mexico observations.

Implications of Composite Sinusoidal Behavior of Distance to Earth.

From our data table of observations (Supplement Table 1), we ran a long-term integration that extends into the next 4,500 years. The integration showed the asteroid's distance to Earth as an approximate composite sinusoidal function of time over the next several hundred years. This vacillating orbit result indicates external gravitational perturbations acting upon the asteroid by other planets.

Closer at hand, though, we noted that within the first few hundred years, the distance generally ranges between 0.8 AU to 4 AU. Around the year 2310, however, the predicted distance between Earth and 1994 PN decreases to about 0.3 AU. Afterwards, close encounters (distance to Earth less than 1 AU) are predicted to show up frequently. The closest encounter we predicted was 0.02 AU away from the Earth in the year 4154 (Figure 4). Although an asteroid at 0.02 AU may not collide with Earth immediately, it is situated at a comparably close distance to Earth (in relation to the remainder of its periodic orbital patterns), and could be perturbed by nearby celestial objects outside the scope of this investigation onto a collision course with Earth. The integration program predicted minimum distances that gradually decrease for the first 300 years with each passing cycle of the asteroid's sinusoidal distance behavior, culminating in the dangerously close encounter in 4147. Thus, it is reasonable to conclude that 1994 PN has a high possibility of colliding with the Earth in the future.

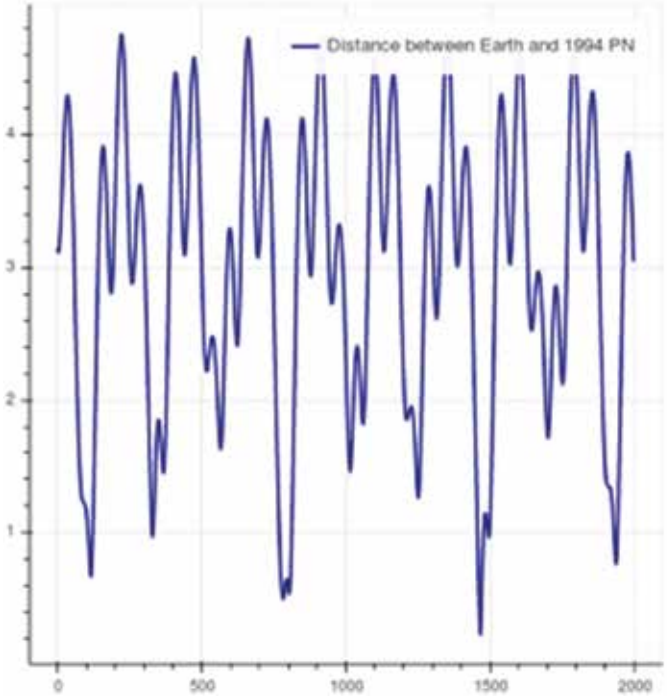

Figure 3. The distance between 1994 PN and Earth shows a periodic pattern. The asteroid move mostly within rage 0.8 to 4 AU. For convenience, we use integers from 0 to 2000 on the x-axis; each increment is 0.1 sidereal day, which is roughly 6 days.

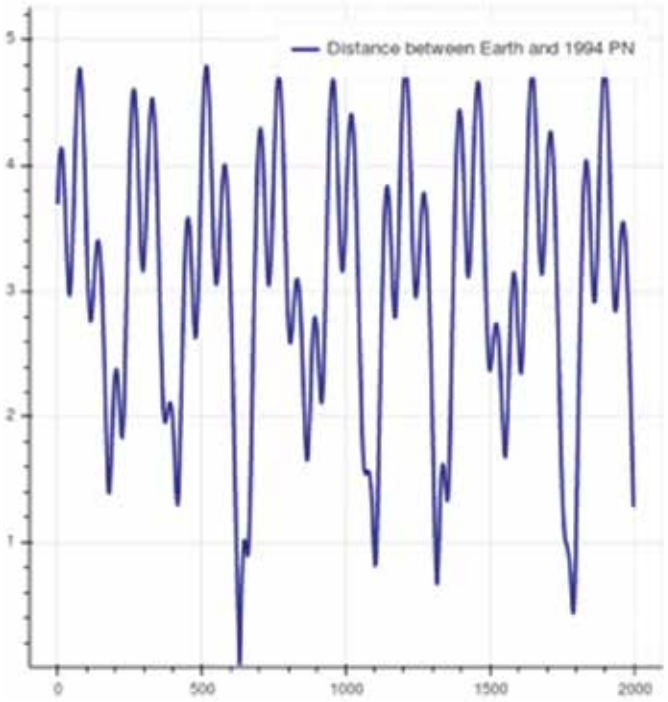

Figure 4. Additionally 2000 data points predicted from April 3958 to January 4713. Around year 4157 (620 on x-axis), the distance is as close as 0.02 AU.

SUPPORTING INFORMATION

I. **Methods:** Method of Gauss.

II. **Supplement Table 1**: Observed RA, Dec, and Apparent Magnitude of Asteroid 1994 PN.

III. **Supplement Table 2**: Comparison of RA, Dec, and Orbit Elements between observed data and JPL Horizons data.

ACKNOWLEDGMENTS.

We would like to thank our Academic Director, Dr. Michael D. Faison, for mentoring our research this summer at YSPA, and Dr. Mary Loveless for helping us edit this paper. We would also like thank Teaching Fellow Jesse Feddersen for helping us with the Python programming and introducing us to data science techniques and Teaching Assistants Daksha Rajagopalan and Alex Thomas for supporting our research.

REFERENCES.

1. T. J. Ahrens, A. W. Harris, Deflection and fragmentation of NEA, *Nature*. 360, 429-433, (1992).
2. E. Blasy, data presented at the Yale Summer Program in Astrophysics, New Haven, CT, 6 August 2016.
3. M. Faison, paper presented at the Yale Summer Program in Astrophysics, New Haven, CT, 6 August 2016.
4. S. Forrest, Genetic Algorithms: Principles of Natural Selection Applied to Computation Genetic Algorithms: Principles of Natural Selection Applied to Computation, *Science, New Series*. 261, 872-878, (1993).
5. S. Pravdo, *et al*. The Near-Earth Asteroid Tracking (NEAT) Program: An Automated System for Telescope Control, Wide-field Imaging, and Object Detection, *The Astronomical Journal*. 117,1616-1633, (1999).
6. S. Ross, "Near-Earth Asteroid Mining," Control and Dynamical Systems, Caltech, *Space Industry Report*. 14 December 2001.
7. M. Shao, *et al*, "Finding Very Small Near-Earth Astroird Using Synthetic Tracking," *The Astrophysical Journal*. 782 (2014).

Amy Dai is a student at Cape Central High School in Cape Girardeau, MO.

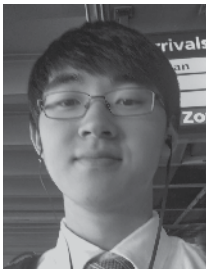

Frank Bu is a student at Baylor School in Chattanooga, TN.

Aaron Kogan is a student at Hopkins School in New Haven, CT.